

A. Aierken, T. Hakkarainen, J. Riikonen, and M. Sopenen. 2008. Transformation of InAs islands to quantum ring structures by metalorganic vapor phase epitaxy. *Nanotechnology*, volume 19, 245304.

© 2008 Institute of Physics Publishing

Reprinted with permission.

<http://www.iop.org/journals/nano>
<http://stacks.iop.org/nano/19/245304>

Transformation of InAs islands to quantum ring structures by metalorganic vapor phase epitaxy

A Aierken¹, T Hakkarainen, J Riikonen and M Sopanen

Department of Micro and Nanosciences, Micronova, Helsinki University of Technology,
PO Box 3500, FIN-02015 TKK, Finland

E-mail: abuduwayiti.aierken@tkk.fi

Received 6 December 2007, in final form 26 March 2008

Published 9 May 2008

Online at stacks.iop.org/Nano/19/245304

Abstract

The transformation of InAs islands to quantum rings (QRs) by metalorganic vapor phase epitaxy is investigated. After covering the InAs islands with a thin GaAs partial capping layer and annealing under tertiarybutylarsine (TBAs) flow, ring-shaped nanostructures with a density of 10^7 – 10^9 cm⁻² are obtained at 500–600 °C. The effects of the growth temperature, annealing process and thickness of the partial capping layer are studied. Optimum values for the annealing time and the partial capping layer thickness were found to be 60–120 s and 0.5–2.0 nm, respectively. Low temperature photoluminescence (PL) emission peaks from islands and QRs grown at 500 °C are observed at 1.04 eV and 1.22 eV, respectively. The annealing temperature affected the QR evolution and the PL emission from the QRs due to the temperature dependence of the diffusion rate of indium atoms.

(Some figures in this article are in colour only in the electronic version)

1. Introduction

In recent years, there has been increased interest in studying quantum ring (QR) structures because of their electrical [1, 2], optical [3] and magnetic [4–6] properties. Due to their ring-like shape, QRs have electronic properties that differ from those of other quantum structures. Experimental observation of Aharonov–Bohm effects [7, 8] and persistent current [9, 10] in QR structures brought more interest to this field. Since the first growth of self-assembled InAs QRs by García *et al* [11], numerous theoretical and experimental studies of QRs have been reported. Different types of growth techniques and materials have been applied to fabricating the QRs. For instance, island-to-ring transformation for In(Ga)As/GaAs [12–14], AlAs/GaAs [15], InAs/InP [16], and GaSb/GaAs [17] materials by covering the islands with a partial capping layer have been reported. In addition, InAs/InP QR formation by As–P exchange [18, 19] or direct formation of InGaAs/GaAs QRs by droplets [20] has also been demonstrated. Furthermore, some potential applications

for In(Ga)As/GaAs QRs in laser devices [21] have been reported. Among the different types of QRs, In(Ga)As/GaAs is probably the most widely studied QR structure material system. However, most of these studies have been done by molecular beam epitaxy (MBE), and the effects of growth conditions on the formation and properties of QRs are rarely reported in detail.

In this paper, we investigate the formation of InAs QRs on GaAs(100) by using metalorganic vapor phase epitaxy (MOVPE). InAs island-to-ring transformation is carried out by covering the InAs islands with a thin GaAs partial capping layer. QR formation is studied over a wide range of growth parameters, and the effects of growth conditions on the surface morphology and optical properties of the QRs have been investigated.

2. Experimental details

The samples were grown on semi-insulating GaAs(100) substrates in a horizontal MOVPE reactor at atmospheric pressure using trimethylindium (TMIn), trimethylgallium (TMGa), and tertiarybutylarsine (TBAs) as precursors for

¹ Author to whom any correspondence should be addressed.

indium, gallium, and arsenic, respectively. A 100 nm thick GaAs buffer layer was grown first at the growth temperature of 650 °C with a V/III ratio of 23. Before the InAs deposition, the reactor temperature was stabilized at the InAs growth temperature T_g (500–600 °C) under TBAs flow to protect the surface. InAs islands were formed by depositing a nominally 1.7 monolayer (ML) thick InAs layer on the buffer layer with a growth rate of 1.5 ML s⁻¹ and a V/III ratio of 10, based on the results of our previous study [22]. After 15 s of stabilization, the InAs islands were transformed into QRs by capping the islands with a 2 nm thick GaAs partial capping layer followed by annealing under TBAs flow. The annealing time, t_a , was 60 s and the annealing temperature, T_a , was the same as the island growth temperature, $T_a = T_g$. After switching off the reactor heating lamp, the TBAs flow was continuously applied during the sample cooling until the temperature had decreased to 300 °C. T_a , t_a and the thickness of the partial capping layer, d_c , were varied to study the effects of the growth conditions. The reference InAs island samples were taken out from the reactor right after the island growth and cooling down under TBAs flow. Samples for the photoluminescence (PL) measurement were covered with a 50 nm thick GaAs barrier layer at the annealing temperature T_a after the QR transformation was completed. The temperatures mentioned in this paper are thermocouple readings and V/III ratios are molar flow ratios.

The morphology of the QRs was characterized using contact-mode atomic force microscopy (AFM). The AFM tips were non-conductive silicon nitride tips with a tip diameter of 20 nm. The low temperature (10 K) continuous-wave PL measurements were conducted by utilizing a diode-pumped frequency-doubled Nd:YVO₄ laser emitting at 532 nm for excitation. A liquid-nitrogen-cooled germanium detector and standard lock-in techniques were used to record the PL spectra.

3. Results and discussion

3.1. Island-to-ring transformation

Before studying the QR transformation, InAs islands, without the partial capping layer, were grown at different temperatures (500–600 °C) for reference. The areal density, average base diameter and average height of the InAs islands are shown in figure 1. When the growth temperature is increased from 500 to 600 °C, the island density decreases from about 10⁹ to 10⁷ cm⁻² (figure 1(a), solid line) and the islands become larger (figure 1(b)). This result follows the mass distribution of the three-dimensional (3D) islands as a function of the growth temperature, as expected [23]. At the growth temperature of 550 °C, the average base diameter and average height of the InAs islands are 100 nm and 36 nm, respectively.

After partial capping and annealing, the InAs islands are transformed into QRs. 2D and 3D AFM images of these QRs grown at different temperatures are shown in figure 2. The areal density of the QRs (shown in figure 1(a), dotted line) is smaller than that of the original islands. The difference is larger when the growth temperature is higher. At 570 °C, the QR density is about one quarter of the island density. In

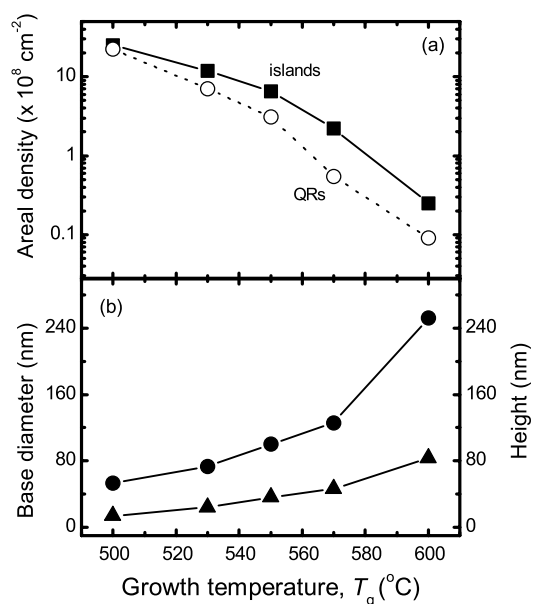


Figure 1. (a) The areal density of InAs islands and QRs, and (b) the average base diameter (●) and height (▲) of InAs islands as a function of growth temperature T_g .

the reference samples, no obvious differences were observed between the areal density of InAs islands with and without the 15 s stabilization. Therefore, we assume the reduction of the QR density to be related to the temperature dependence of the indium atom diffusion during the annealing of the partially capped islands, which will be discussed in detail in the next section. Due to the large size of the islands, most of the islands were not completely transformed into rings when the growth temperature was 600 °C (figure 2(e)).

Island-to-ring transformation results in significant changes in the height and lateral dimension of the QRs compared to those of the initial islands. Cross-sectional profiles, in the [110] and $[1\bar{1}0]$ directions, of a typical QR grown at 550 °C are shown in figures 3(a) and (b). The [110] and $[1\bar{1}0]$ crystal directions of the QR are shown in figure 3(c). The lateral distance of the outer and inner edge of the rim and rim height are different for [110] and $[1\bar{1}0]$ directions. Compared to the average size of a typical island (figure 3(d)) grown at the same temperature, the lateral distance of the QR is increased over 2 times and the height is decreased about 6–10 times.

Similar ring characteristics were observed for all the other QRs grown at different temperatures. Due to the different size of the initial islands at different growth temperatures, the lateral dimension of the QRs is increased when the growth temperature increases. However, the camel-hump shape of the QRs is more obvious at lower growth temperatures (figures 2(a) and (b)) while the QRs are closer to a perfect ring shape at higher growth temperatures (figures 2(c) and (d)). The main reason for the anisotropy of the rings is the different diffusion rate of indium atoms in different directions [14].

3.2. Ring evolution

The mechanism of island-to-ring formation has been explained by using both kinetic and thermodynamic models [24–26]. It

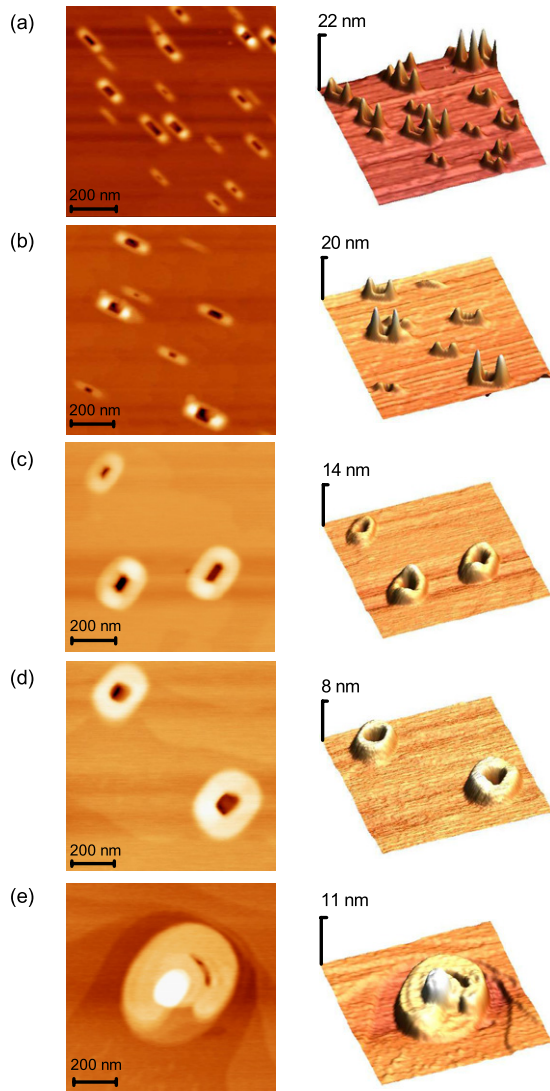


Figure 2. 2D and 3D AFM images of InAs QRs fabricated at different temperatures: (a) 500 °C, (b) 530 °C, (c) 550 °C, (d) 570 °C, and (e) 600 °C. $d_c = 2$ nm, $t_a = 60$ s. The size of all the images is $1 \mu\text{m} \times 1 \mu\text{m}$. Please note the difference in the vertical scale.

has been concluded that the overgrowth of InAs islands with GaAs is a non-equilibrium process. The partial capping layer does not cover the islands because the strain makes the apexes of the islands unfavorable locations for GaAs growth, i.e., the island apexes remain uncovered [24]. The kinetic model is based on the different surface diffusion rates of group III atoms. Indium atoms are more mobile at typical annealing temperatures, and gallium atoms, on the other hand, experience only limited diffusion after they have been incorporated into the crystal lattice [25]. Consequently, the indium atoms on the top of an InAs island diffuse outward and a ring-shaped (In–Ga)As alloy rim with a void in the center of the initial island will be formed. Furthermore, the diffusion of indium atoms is much faster along the $[1\bar{1}0]$ direction than along the $[110]$ direction [25], which is attributed to the chemical reactive anisotropy of group III migrating atoms [14]. As a result, the QRs are not completely round-shaped but elongated in the $[110]$ direction and have a camel-hump-like appearance.

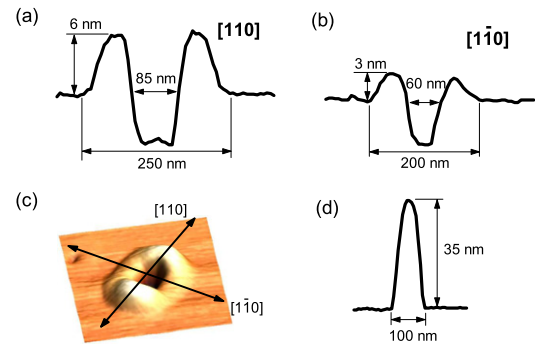


Figure 3. (a) $[110]$ and (b) $[1\bar{1}0]$ cross-sectional profile of a typical QR grown at 550 °C by covering 1.7 ML InAs islands with a 2 nm GaAs partial capping layer. (c) 3D AFM images of a QR with the crystal directions indicated. (d) The cross-sectional profile of an InAs island grown at 550 °C.

According to the AFM images shown in figures 2 (a)–(d), it can be seen that the diffusion rate of the indium atoms not only depends on the temperature but also on the direction. Below 530 °C, the diffusion rate of the indium atoms is much slower in the $[110]$ direction than in the $[1\bar{1}0]$ direction. Above 550 °C, the diffusion rate is comparable in both directions. The high temperature may also be one possible reason for the reduction of the areal density of the QRs. At higher annealing temperature, the mobility of indium atoms is much higher and equivalent in all directions. Under this condition, small islands could become larger in lateral dimension and almost flat, or overlapped with the neighbor islands.

The thermodynamic model, on the other hand, suggests that the partial capping layer induces a change in the balance of surface free energy and, consequently, an outward pointing force is created [24, 26]. As a result, the system finds a new equilibrium in a ring structure via material redistribution. However, it has been concluded that the island-to-ring transformation is promoted by both kinetic and thermodynamic mechanisms [24].

3.3. Effect of growth conditions on ring evolution

Since both kinetics and thermodynamics play important roles in the island-to-ring evolution, the annealing process and the thickness of the partial capping layer affect the ring formation significantly. The effects of annealing time were studied by varying the annealing time t_a from 10 to 120 s at $T_g = T_a = 550$ °C. Figure 4(a) shows the island-to-ring transformation completion percentage as a function of t_a . When $t_a = 10$ s, only 40% of islands are transformed into QRs. After 30 s of annealing, the completion rate has increased to 80%, but some bigger islands still remain not fully converted (figure 4(b)). When the annealing time is in the range of 60–120 s, the completion percentage is over 90%. Longer t_a did not show significant additional effects.

The effect of partial capping layer thickness was studied by varying d_c from 0.5 nm to 5.0 nm while keeping T_a and t_a at 550 °C and 120 s, respectively. Figure 5 shows the 3D AFM images of the QRs grown with different d_c . Well-distributed, relatively homogeneous QRs were observed when the partial

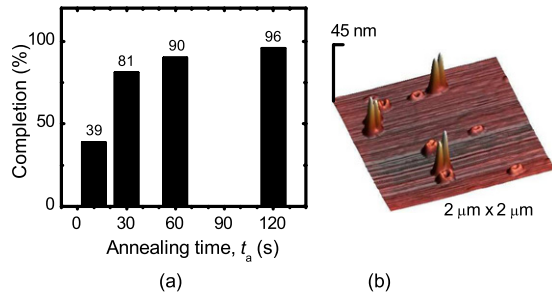


Figure 4. (a) Island-to-ring transformation completion percentage as a function of annealing time, t_a ($T_g = T_a = 550^\circ\text{C}$, $d_c = 2\text{ nm}$). (b) 3D AFM image of the QRs with $t_a = 30\text{ s}$.

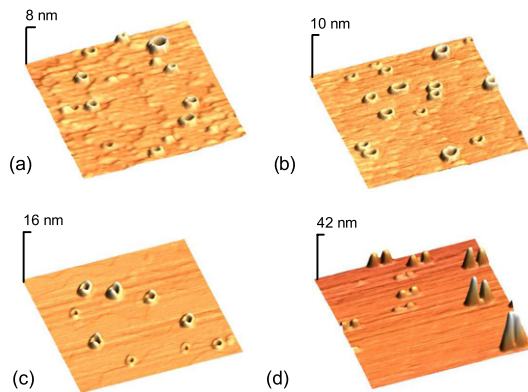


Figure 5. 3D AFM images of QRs fabricated with different partial cap layer thicknesses d_c : (a) 0.5 nm, (b) 1 nm, (c) 2 nm, and (d) 5 nm. $T_g = T_a = 550^\circ\text{C}$, $t_a = 120\text{ s}$. The size of all the images is $2\ \mu\text{m} \times 2\ \mu\text{m}$. Please note the difference in the vertical scale.

capping layer is between 0.5 and 2 nm. The use of a 5 nm thick capping layer leads to uncompleted ring transformation. The surface forces are probably too small to rupture the island when such a thicker capping layer is used. In this case, not only the surface forces but also the full free energy balance should be taken into account [26]. When one compares figure 5(d) with figure 4(b), it can be concluded that both a thicker cap layer and shorter annealing time produce the same kind of suppression for QR evolution.

Besides the annealing time, the annealing temperature also affects QR formation significantly. Figures 6(a)–(c) show the comparison of the [110] cross-sectional profiles of a typical QR grown at 500°C but annealed at 500°C , 550°C , and 570°C , respectively. Figure 6(d) shows the temperature sequence of the QR samples in figures 6(a)–(c). It can be clearly seen that the camel-hump-like shape disappears and the QRs are less elongated when annealed at higher temperature (figure 6(e)). Compared to the QRs annealed at 500°C , the height of the QR rim in the [110] direction is decreased from 11 to 5 nm and to 3 nm when the annealing temperature is 550°C and 570°C , respectively. The diameter of the QR measured from the outer edge is not affected. In the $[1\bar{1}0]$ direction, on the other hand, the height of the rim is comparable ($\sim 3\text{ nm}$) in these three cases and the lateral distance is closer to that of the [110] direction when the annealing temperature is higher (figures not shown). Furthermore, it seems that the void is somewhat deeper at

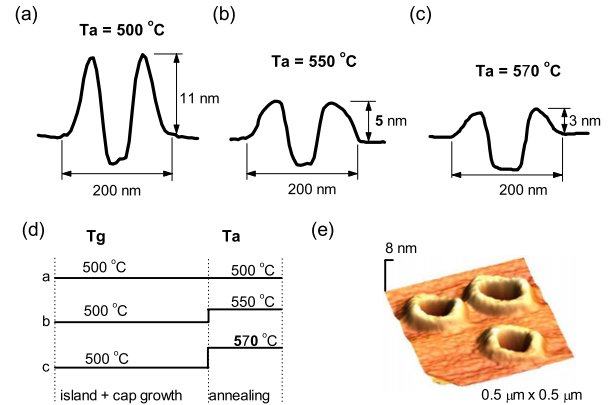


Figure 6. Comparison of [110] cross-sectional profiles of QRs, grown at $T_g = 500^\circ\text{C}$, annealed at different T_a : (a) 500°C , (b) 550°C , and (c) 570°C ($d_c = 2\text{ nm}$, and $t_a = 60\text{ s}$). (d) Temperature sequence during fabrication of the QR samples shown in (a), (b) and (c). (e) 3D AFM image of the QRs grown at $T_g = 500^\circ\text{C}$ and annealed at $T_a = 570^\circ\text{C}$.

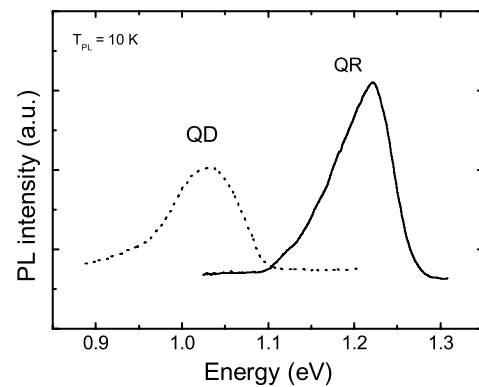


Figure 7. Low temperature (10 K) PL intensities of buried InAs islands (QDs) and QRs. 1.7 ML InAs islands were grown at $T_g = 550^\circ\text{C}$, and QRs were transformed from these islands by using $d_c = 2\text{ nm}$, $t_a = 60\text{ s}$ and $T_a = 550^\circ\text{C}$. The laser excitation density is 30 W cm^{-2} .

higher annealing temperatures, which might be caused by the removal of the intermixed lower island interface. As discussed in the previous section, the temperature dependence of the diffusion rate of indium atoms is the main factor behind the changes of the QRs annealed at different temperature.

3.4. Optical properties of QRs

Low temperature PL spectra from the buried InAs islands and QRs are shown in figure 7. The InAs islands were formed by depositing a nominal 1.7 ML thick InAs layer at $T_a = 550^\circ\text{C}$ and QRs were transformed from these InAs islands by using a 2 nm thick partial capping layer and annealing under TBAs for 60 s at $T_a = 550^\circ\text{C}$. Both samples were covered with a 50 nm thick GaAs barrier layer. PL peaks from QDs and QRs were observed at 1.04 eV and 1.22 eV with the full width at half maximum (FWHM) of 87 meV and 75 meV, respectively. The PL peak of the QRs is about 180 meV blue-shifted with respect to the QD peak.

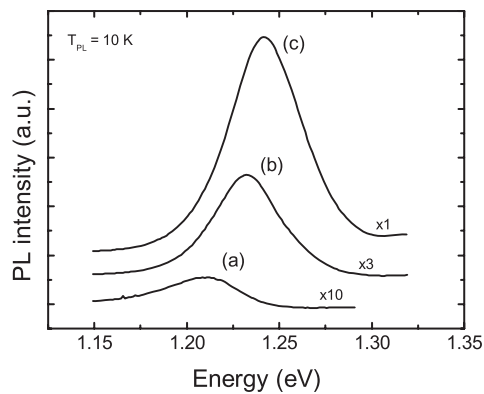


Figure 8. Low temperature (10 K) PL intensities of buried QRs annealed at different T_a : (a) 500 °C, (b) 550 °C, and (c) 570 °C. The QR transformation parameters are the same as shown in figure 6. The laser excitation density is 30 W cm⁻².

Figure 8 shows the low temperature PL spectra from QRs annealed at different annealing temperature T_a . The other growth parameters for the QRs were same as described in figure 6. When T_a is increased from 500 to 570 °C, the PL emission peak from the QRs is blue-shifted from 1.21 to 1.24 eV. This indicates that at higher annealing temperature more indium atoms diffused from the islands, so the In composition in the InGaAs rim became smaller. This result agrees with the surface morphological properties of the QRs shown in figure 6. Moreover, it was observed that the PL intensity of the QRs in figure 8(c) is more than ten fold higher compared to that of in figure 8(a). We assume that this higher PL intensity was caused by the high crystal quality of the GaAs barrier layer grown at higher growth temperature [27].

4. Conclusion

In summary, the transformation of InAs islands into QRs by MOVPE was investigated. The transformation was carried out by covering the 1.7 ML InAs islands with a 2 nm thick GaAs partial capping layer and annealing under TBAs flow for 60 s. In the temperature range 500–600 °C, ring-shaped QR nanostructures with a density of 10⁷–10⁹ cm⁻² were obtained. The evolution of the QRs and their properties were discussed by using the kinetic and thermodynamic models given by Lorke *et al* [24–26]. The areal density and dimensions of the QRs were different from those of the initial islands. The QRs were not completely round-shaped but elongated in the [110] direction due to the faster diffusion of indium atoms along the [1 $\bar{1}$ 0] direction. The effects of growth conditions were studied by changing the annealing time and the partial capping layer thickness as well as the annealing temperature. Optimum values for the annealing time and the partial capping layer thickness were found to be 60–120 s and 0.5–2.0 nm, respectively. Low temperature PL measurement results showed that there is about 180 meV blue-shift of PL

emission from QRs with respect to the original QDs. The annealing temperature affected the QR evolution and the PL emission from the QRs due to the temperature dependence of the diffusion rate of indium atoms.

Acknowledgments

One of the authors (A Aierken) acknowledges financial support from the China Scholarship Council. T Hakkarainen acknowledges financial support from the Academy of Finland.

References

- [1] Llorens J M, Trallero-Giner C, García-Cristóbal A and Cantarero A 2002 *Microelectron. J.* **33** 355
- [2] Filikhin I, Suslov V M and Vlahovic B 2006 *Physica E* **33** 349
- [3] Warburton R J, Schäfflein C, Haft D, Bickel F, Lorke A, Karrai K, García J M, Schoenfeld W and Petroff P M 2001 *Physica E* **9** 124
- [4] Haft D, Schulhauser C, Govorov A O, Warburton R J, Karrai K, García J M, Schoenfeld W and Petroff P M 2002 *Physica E* **13** 165
- [5] Voskoboynikov O and Lee C P 2004 *Physica E* **20** 278
- [6] Planelles J, Jaskólski W and Aliaga J I 2001 *Phys. Rev. B* **65** 033306
- [7] Keyser U F, Fühner C, Haug R J, Wegscheider W, Bichler M and Abstreiter G 2003 *Phys. Status Solidi b* **238** 331
- [8] Kähler D, Kunze U, Reuter D and Wieck A D 2003 *Physica E* **17** 284
- [9] Chakraborty T and Pietiläinen P 1994 *Phys. Rev. B* **50** 8460
- [10] Orellana P A and Pacheco M 2005 *Phys. Rev. B* **71** 235330
- [11] García J M, Medeiros-Ribeiro G, Schmidt K, Ngo T, Feng J L, Lorke A, Kotthaus J and Petroff P M 1997 *Appl. Phys. Lett.* **71** 2014
- [12] Takehana K, Pulizzi F, Patane A, Henini M, Main p C, Eaves L, Granados D and García J M 2003 *J. Cryst. Growth* **251** 155
- [13] Granados D and García J M 2003 *J. Cryst. Growth* **251** 213
- [14] Granados D and García J M 2003 *Appl. Phys. Lett.* **82** 2401
- [15] Lee B C and Lee C P 2004 *Nanotechnology* **15** 848
- [16] Raz T, Ritter D and Bahir G 2003 *Appl. Phys. Lett.* **82** 1706
- [17] Kobayashi S, Jiang C, Kawazu T and Sakaki H 2004 *Japan. J. Appl. Phys.* **43** L662
- [18] Poole P J, Williams R L, Lefebvre J and Moisa S 2003 *J. Cryst. Growth* **257** 89
- [19] Sormunen J, Riikonen J, Mattila M, Tiilikainen J, Sopenan M and Lipsanen H 2005 *Nano Lett.* **5** 1541
- [20] Gong Z, Niu Z C, Huang S S, Fang Z D, Sun B Q and Xia J B 2005 *Appl. Phys. Lett.* **87** 093116
- [21] Suárez F, Granados D, Dotor M L and García J M 2004 *Nanotechnology* **15** S126
- [22] Aierken A, Hakkarainen T, Sopenan M, Riikonen J, Sormunen J, Mattila M and Lipsanen H 2007 *Appl. Surf. Sci.* **254** 2072
- [23] Solomon G S, Trezza J A and Harris J S 1995 *Appl. Phys. Lett.* **66** 991
- [24] Lorke A, Luyken R J, García J M and Petroff P M 2001 *Japan. J. Appl. Phys.* **40** 1857
- [25] Lorke A, Blossey R, García J M, Bichler M and Abstreiter G 2002 *Mater. Sci. Eng. B* **88** 225
- [26] Blossey R and Lorke A 2002 *Phys. Rev. E* **65** 021603
- [27] Ohtsubo R and Yamaguchi K 2003 *Phys. Status Solidi c* **0** 939